Bibliographical reference

High-Resolution Imaging of Sound Sources in Free Field Using a Numerical Time-Reversal Sink, Éric Bavu and Alain Berry, Acta Acustica **vol. 95** (Number 4), 2009, pp. 595-606

DOI

https://doi.org/10.3813/AAA.918188

ACTA ACUSTICA UNITED WITH ACUSTICA
Vol. 95 (2009) 595 – 606

DOI 10.3813/AAA.918188

High-Resolution Imaging of Sound Sources in Free Field Using a Numerical Time-Reversal Sink

Éric Bavu*, Alain Berry
Groupe d'Acoustique de l'Université de Sherbrooke, 2500 boul. de l'Université, Sherbrooke, Québec, J1K 2R1, Canada. bavu@lam.jussieu.fr

Summary

Numerous practical applications – such as non destructive evaluation of industrial structures, acoustic characterization of musical instruments, and acoustic mapping of sound sources in a known propagation medium – involve source detection and characterization. In the past, this problem has been investigated using different beamforming and backpropagation methods. In this work, a new technique, based on the time reversal sink concept, is used to detect active sound sources with a limited number of measurement points. The theory and application of super-resolution focusing of sound and vibration using a time-reversal sink (TRS) have been studied, both in ultrasonic regime and in audible range. A high-resolution imaging technique based on a numerical time reversal sink has recently been developed by the authors for vibrational imaging of active sources in a dispersive medium. In this paper, the numerical time reversal sink imaging technique is adapted to the case of high-resolution acoustic imaging of active sound sources in a three-dimensional free field. This technique allows high-resolution imaging and provides a new method of characterization and detection of sound sources. All results show the high resolution imaging capabilities of this new technique when compared with classical time-reversal (TR) backpropagation. More than simply detecting the position of the acoustic source, this technique allows to detect the size of the active sources. This technique provides an alternative to other imaging and source detection techniques, such as three-dimensional acoustic holography and beamforming.

PACS no. 43.28.Js, 43.30.Bp, 43.30.Pc, 43.30.Gk, 43.60.Jn, 43.60.Lq, 43.60.Tj

1. Introduction

In many practical situations, it is necessary to localize and characterize an audible sound source using a few sensors. Existing techniques such as three-dimensional acoustic holography [1], beamforming and matched-field processing [2] involve an array of sensors and the knowledge of the propagating medium. Time reversal (TR) techniques are also widely used to locate active sources and scatterers [3, 4, 5, 6, 7]. Time reversal and its derivatives have been shown to be an effective localization technique in audible frequency range [8]. However, since time-reversal technique is an interference phenomenon leading to diffraction effects between diverging waves and converging waves around the focal spot, the imaging resolution produced by time-reversal cannot be smaller than half a wavelength, even if the source is pointlike [9]. More recently, a new technique based on the concept of numerical time reversal sink (TRS) has been introduced by the authors, in order to achieve high-resolution of active vibrational sources in a plate [10]. In the present article, the numerical TRS technique is applied to the case of high resolution acoustic imaging of active sound sources in free field. This technique allows high-resolution imaging and provides a new method of characterization and detection of active sound sources in free field. In contrast with most other existing techniques involving beamforming, classical time-reversal, or time of arrival detection, TRS provides detailed information on the boundaries of the active source instead of just localizing the center of this source.

The time-reversal sink has been first introduced by Fink *et al.* [9] and by Rosny *et al.* [11, 12] in ultrasonic range with Lamb waves on a chaotic silicon plate. This technique allows high quality subwavelength focusing and has been shown to enhance the limit of resolution of focusing when compared to classical time-reversal (TR) backpropagation [11]. The technique also proved to be very effective, even with a single channel time-reversal mirror (TRM) in a reverberant or chaotic environment [13, 14, 15]. In audible range, the sound focusing capabilities of an experimental TRS have been studied both in a damped and reverberant environment, showing that a reverberant environment allows accurate resolution focusing using a limited number of transducers if the diffuse field component of the forward propagation is recorded and time-reversed. However, as stated in [10], the numerical TRS imaging technique requires an accurate computation of the backpropagation in

Received 18 August 2008,
accepted 18 March 2009.

* Also at: UPMC Univ Paris 06, U.M.R. C.N.R.S. 7190, IJLRA/LAM, 11, rue de Lourmel, 75015 Paris, France

the background medium. Computing the acoustic propagation after the mixing time in a reverberant room is an impossible task to achieve in terms of accuracy and computation time [16, 17, 18]. Thus, this work presents the numerical TRS imaging method in free field only.

We consider the following situation: an arbitrary number N of unknown sources emit an acoustic signal $s_i(t)$ ($i \in [1 : N]$) in an infinite background medium. The acoustic wave $\psi(\vec{r}, t)$ is recorded on a control surface at M control points using a sensor array. Due to linearity, the signal measured at the mth control point can be written as follows ($m \in [1 : M]$):

$$\psi(\vec{r}_m, t) = \sum_{i=1}^{N} G(\vec{r}_i, \vec{r}_m; t) * s_i(t), \qquad (1)$$

where $s_i(t)$ is the source signal, $G(\vec{r}_i, \vec{r}_m; t)$ is the Green's function between the ith source and the mth control point (* denotes the convolution in the time domain).

The second step consists in a simulated backpropagation of the time reversed signals $\psi(\vec{r}_m, -t)$ reemitted at each control point using a time domain finite difference (FDTD) algorithm in a fictive medium approaching the characteristics of the real background medium. At the end of this computation step, the position of each source can be detected by using peak detection in both space and time domains[1]. This detection corresponds to the localization of active sources by numerical TR backpropagation, but the resolution is limited by diffraction effects between converging waves and diverging waves around the focal spots [19] and depends on the wavelength of the waves emitted by the N sources. At this stage of the process, there is no information on the size of the N sources. The last step of the process consists in emitting the superposition of N numerical TRS in the fictive medium simultaneously to the M time reversed signals of the previous step. The N TRS are located at the positions of the active sources detected at the end of the second step. This simulation is computed using the same FDTD algorithm than the one used in the second step.

As stated in [13] and [10], the resolution of imaging does not depend on the wavelength because diffraction effects are supressed by the TRS process, and the focal spot width equals $\max(\phi_{\text{source}}; \phi_{\text{sink}})$, ϕ_{source} being the size of the initial source and ϕ_{sink} the size of the sink. In our process, the source used to create the numerical sink is an ideal point source. Thus, the resolution of the TRS imaging process is exactly the size of the initial source and allows access to details on the spatial extent of the sound source, even in situations where the size of the source is smaller than half the wavelength. In the following, these properties are experimentally demonstrated. In a first Section, the experimental setup and the numerical algorithm for backpropagation and TRS simulation are detailed. Then, a numerical proof of principle is presented in order to show the capabilities of this new imaging technique in audible range. In a third Section, the results of TRS imaging experiments are presented and compared to the localization obtained using numerical TR backpropagation, in order to show the high-resolution capabilities of this new technique in real situations. The advantages of this technique when compared to classical active source localization techniques are also discussed.

[1] Alternatively, a high-resolution source localization technique, such as MUSIC [19] can be used

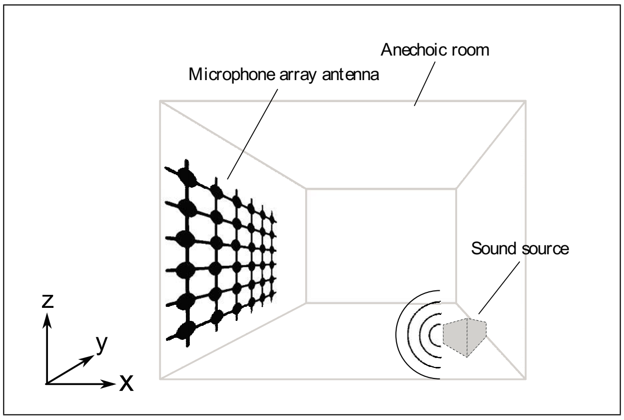

Figure 1. Experimental setup: The positions of active sources and control points shown are for illustration purpose.

2. Experimental setup and methods

2.1. Experimental setup

In this article, we consider the following situation, illustrated in Figure 1. An arbitrary configuration of sound sources emits an impulsive signal in a 3.1×2.5×3.0 m anechoic room. Experimentally, the sound sources are 5.08 cm diameter / 15-Watt transducers (Aurasound NSW2-326-8A loudspeakers) mounted on a closed 4.8×13 cm cylindrical cavity. A two-dimensional microphone antenna (6×6 Panasonic WM61A omnidirectional back electret condenser microphones with constant inter-microphone spacing of 75 mm) is used to measure the acoustic pressure at 36 control points in the anechoic environment. In order to guarantee exact synchronisation of the measurements at several points, the source signals are generated using Matlab software and emitted using a Echo Audiofire12 soundcard. The acoustic pressure measured at the control points is acquired using 3 Echo AudioFire soundcards and Matlab, synchronised via worldclock. This experimental setup allows a measurement bandwith of [25 Hz–15 kHz] and a sampling frequency of 88.2 kHz. These measurements are then used as inputs to the simulation to process the time-reversal backpropagation in the anechoic room, simplified as a free field situation.

2.2. Numerical time-reversal sink method: high-resolution imaging

In order to achieve high-resolution imaging of the active sound sources in free field, a numerical time reversal sink is applied in the simulated background medium. This numerical TRS is based on the general principles described in [10], [11] and [13]. As stated in [13], the signal to be emitted by the numerical time-reversal sink is extracted from the pressure field previously computed in the classical TR step. This signal corresponds to the sound pressure (without any normalization process) at the focal point located by using classical TR and peak detection. This signal is then emitted by a numerical pointlike source at the same position, simultaneously to the time reversal mirror signals in order to overcome the apparent failure around the source position in the time reversal process and supress the diffraction effects. In the case of a single sink, the wave emitted by the time-reversal sink can be written as

$$\psi_{\mathrm{TRS}}(\vec{r}_m, t) = G(\vec{r}_s, \vec{r}; t) * s_{\mathrm{TR}}(t), \tag{2}$$

where $s_{\mathrm{TR}}(t)$ is the time-reversed signal at the focus point extracted from the TR computation, and $G(\vec{r}_s, \vec{r}; t)$ is the Green's function between the source at position $\vec{r}_s$ and a receiver at position $\vec{r}$.

TRS method has proven to achieve high resolution sound and vibration focusing, but as stated in [13], implementing a TRS may not be convenient in practice: it involves additional physical sources in the wavefield, collocated with the target position, and whose finite size can limit the spatial resolution obtained in the focusing process. In contrast, the *numerical* TRS used here involves in the *imaging* process a point-like sound source, so that the resolution corresponds to the size of the initial unknown source, if the numerical space step is smaller than its size. Thus, besides being able to locate the active sources, the numerical TRS imaging process allows the reconstruction of spatial details of these sources.

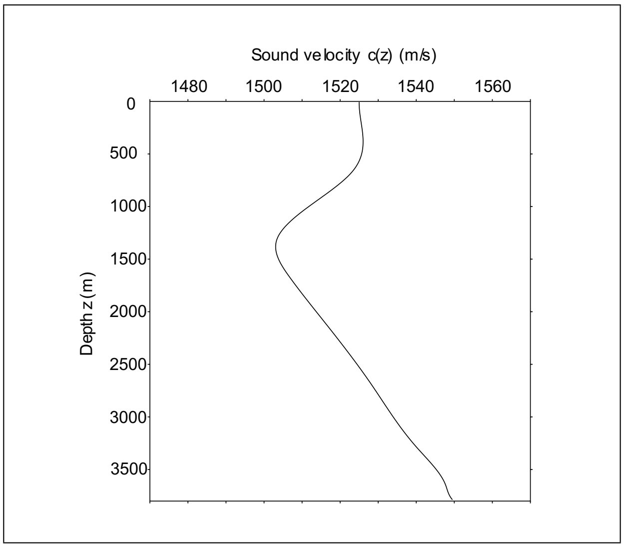

Figure 2. Sound velocity profile used in the numerical experiment.

3. Numerical methods and numerical proof of concept

3.1. Time reversal simulated backpropagation

The algorithm used to compute the TR backpropagation consists in the modeling of the wave propagation in free field conditions. This algorithm is coded in C language using finite difference in the time domain (FDTD) and the simulations are performed on a parallel cluster supercomputer (872 3.2 GHz Intel processors, 3064 Gflops peak performance) in order to reduce the computation time. The code is flexible and cross-platform, and can be compiled on any other architectures. The propagation algorithm is general and can handle spatially varying properties of the propagation medium, as is the case for long range underwater or geophysical applications. The homogeneous medium being a simplification of the layered medium, the same algorithm can be used for different applications with a minimal change in the physical parameters used in the simulation process. Since the propagation takes place in an open space, the acoustic pressure must verify the Sommerfeld boundary condition. The acoustic propagation equation in the medium is discretized in both space and time domains using FDTD. The explicit numerical scheme that was chosen is of fourth order in time and fourth order in space (4-4 explicit centered scheme). The fourth order approximation in space is done by using a composition of fourth-order approximations of the divergence and gradient operators in wave propagation equation. These approximations have good positivity and stability properties [20, 21]. However, a 4-4 centered scheme (even uncentered) leads to unconditionnaly unstable schemes [22] . Therefore, we used a very efficient alternative in order to approach the acoustic wave equation: the modified equation approach (for more information, see [23] and [21]) which has been shown to provide remarkable properties of stability and accuracy [21]. The Sommerfeld condition in the free field is approached by using higher order absorbing boundary conditions [24], in order to compute the acoustic propagation in a numerical space-limited box inside an open space medium without inducing numerical reflections on the fictive boundaries of the box [24, 25]. This method involves Padé approximations and a wide angle approximation involving a rational function paraxial approximation on each facets, edges, and vertex of the parallelipipedic calculus box [24, 26]. This algorithm allows a reliable, fast, stable, and accurate modelization of the acoustic propagation in open space in a layered medium (the isotropic case being a simplification of this model). In the case of a homogeneous free-field configuration, the open medium Green's function can of course be used to model the acoustic propagation instead of the FDTD scheme. Nevertheless, being based on time reversal, which is a powerful adaptative method, the numerical time reversal sink method can be applied to heterogeneous and anisotropic propagation media, and the numerical simulation has been used in this work in order to be applicable in more general cases.

The simulation is first used to compute the TR backpropagation of the signals measured on the microphone

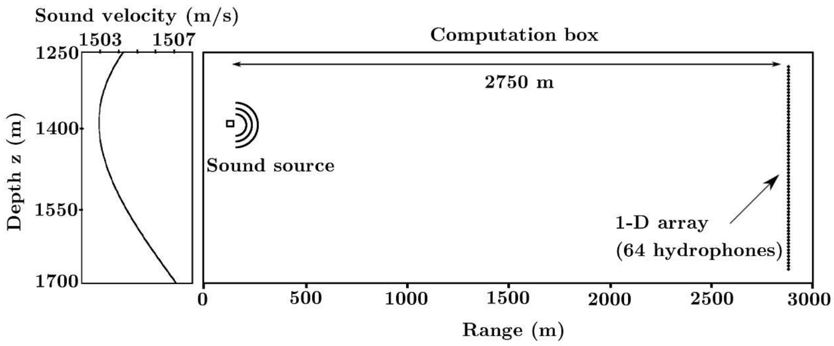

Figure 3. Computationnal configuration for the acoustic source imaging in deep ocean channel.

antenna, giving access to the time-reversed pressure field. If the sources are well resolved in space, a spatio-temporal maximum detection also provides the position of the sources to be imaged. If the sources are non well resolved in space, high resolution localization methods, such as MUSIC or ESPRIT can be used (see Section 4.2.2). The numerical TRS step is necessary to have access to the characteristics of the sources, since classical TR methods are limited by diffraction effects. The numerical time-reversal sink is used to overcome this diffraction limit and to have access to the geometrical characteristics of the sources.

3.2. High-resolution imaging of acoustic sources in deep water channel using numerical TRS: proof of concept

Time reversal acoustics has been shown to be an efficient technique to focus sounds in the ocean [27, 28, 29]. The speed of sound in seawater depends on depth, temperature, and salinity. This corresponds to the layered propagation medium simulation detailed in the previous Section. A typical sound velocity profile is presented on Figure 2. One region of particular interest in ocean is the deep water channel, often called SOFAR (Sound Fixing And Ranging) channel, which acts as a waveguide [30]. The SOFAR channel is a horizontal layer of water in the ocean centered around the depth at which the speed of sound is minimum.

In the numerical experiment, a pointlike sound source, located at the center of the deep water channel ($z_s = -1390$ m, $x_s = 130$ m, corresponding to the minimum of the velocity profile) emits a 2.5-cycles Blackman windowed sinusoid at several frequencies, from 500 Hz to 7500 Hz. A 1-D receiver array (64 hydrophones, spaced by 3 m in the vertical direction) is located at a distance of 2750 m from the sound source (see Figure 3). This particular configuration has been chosen in order to reduce the computation time for this proof of concept. At 500 Hz, the SOFAR channel allows hundreds of kilometers of transmission ranges because of its physical properties [30]. However, for this particular numerical experiment, we have chosen to compute the numerical TRS imaging for a 3000 × 15000 × 100000 finite difference grid with 30 cm spatial sampling, that is, a 90 m × 450 m × 3000 m computational domain in the width, depth and length directions respectively. This configuration has been chosen in order to limit the computation time to 300 minutes. For real applications at larger ranges, this technique remains exactly the same, except the computation time is proportional to the number of space computation points.

The acoustic field received by the array of 64 hydrophones is then time reversed and backpropagated in the SOFAR channel (Figure 4).

Figure 4 shows the results of localization obtained using numerical TR backpropagation of the sound sources at central frequencies of 1500 Hz, 3000 Hz and 5000 Hz. Each figure shows an inverted gray scale image and an a mesh showing the squared acoustic pressure in the SOFAR channel using TR at the instant of focus. The instant of focus was determined using a detection of the absolute maximum of the acoustic pressure over time and position in the computational box. The circles superposed on the images indicate the classical half-wavelength diffraction limit that bounds the resolution of the TR reconstruction. This diffraction effect between the converging and the diverging waves around the focal spots prevents access to the physical size of the source (which, for this numerical experiment, is point-like).

The same numerical experiment has been repeated using the numerical TRS technique. In this case, the time-reversal sink is exactly collocated with the sound source center. Figure 5 shows that using the numerical TRS allows to achieve high-resolution (i.e. subwavelength) imaging of the active source in the deep water channel.

The spatial resolution using TRS does not depend on the frequency of the signal emitted by the active sources and results in high-resolution imaging of the acoustic source, even at low frequency (see Figure 6). The images obtained using TRS in this numerical experiment show that the pointlike source is well reconstructed, and confirms the properties of TRS imaging detailed in the previous Section. In this ideal numerical case, the active source is a numerical pointlike source. Thus, the TRS method provides a pointlike image of the source without degrading the imaging quality even when the frequency is low, whereas the localization obtained using numerical TR backpropagation provides a frequency-dependent resolution because of the diffraction effects. The TRS images show both better resolution and contrast than the TR images, as predicted by the theory and experiments previously published for the focus-

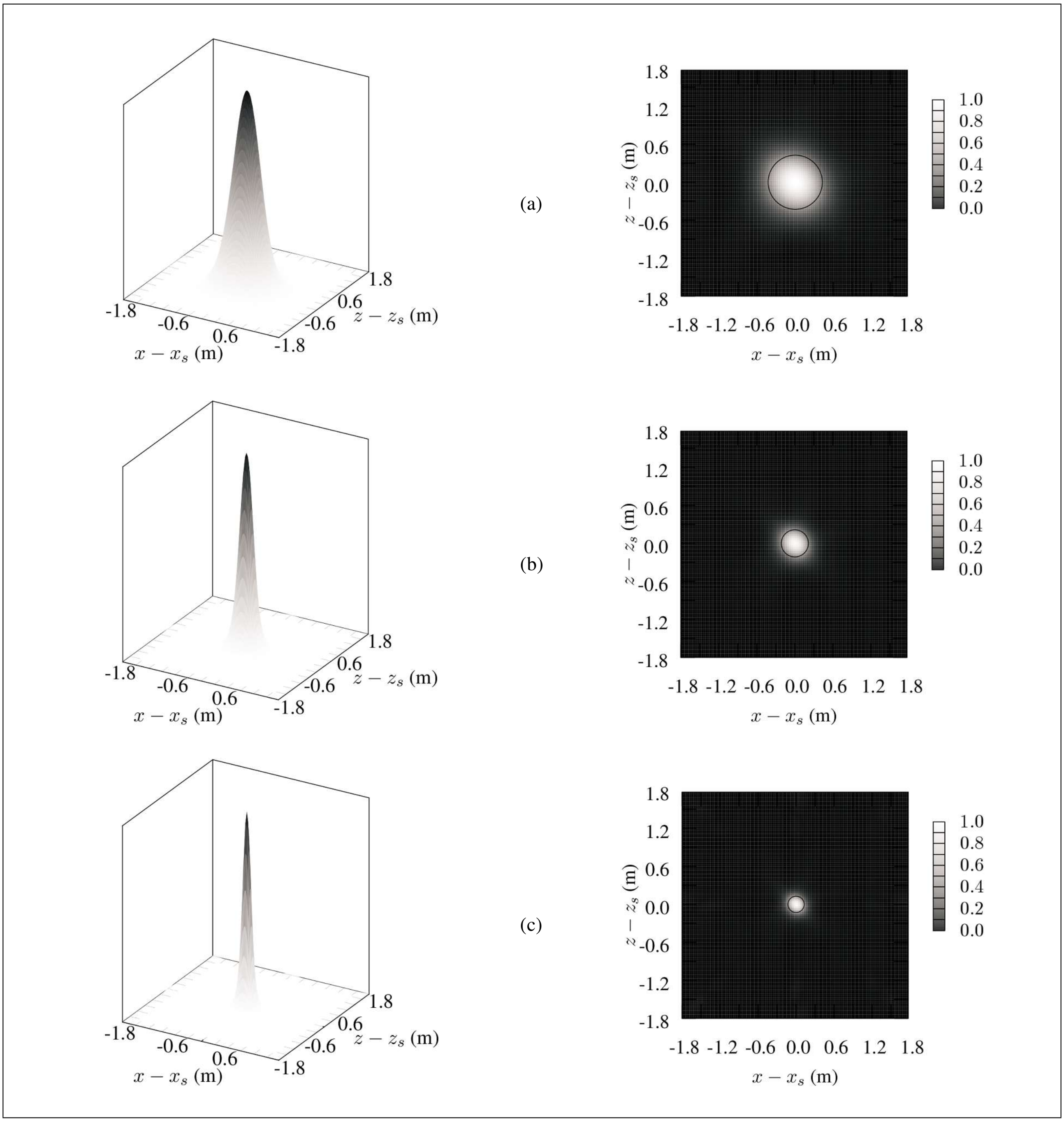

Figure 4. Localization of a underwater pointlike sound source in the SOFAR channel using numerical time reversal backpropagation at central frequencies of (a) 1500 Hz, (b) 3000 Hz, and (c) 5000 Hz. Left: squared acoustic pressure. Right: Source localization (grayscale) compared to the theoretical limit of resolution (circles).

ing TRS [10, 11, 13]. In the case of a pointlike source, the limit of resolution with the TRS technique corresponds to the space sampling in the numerical model of the propagation medium. Figure 6 shows that the limit of resolution (defined as the -3dB focal spot width) obtained using numerical TR backpropagation is about 1.35 larger than the theoretical half wavelength diffraction limit in this configuration.

This can be explained by the fact that the aperture of the TRM used in this numerical experiment is small and that the hydrophone array does not satisfy the half-wavelength spatial sampling. Nevertheless, this configuration corresponds to those used in real underwater experiments [27] and takes into account the amount of hardware classicaly available for such experiments. It is also important to note that the waveguide configuration of the SOFAR channel greatly enhances the resolution available with this hydrophone array configuration [29]. The TR focusing being diffraction limited, the spatial resolution is decreased when the excitation frequency decreases. In applications where the spatial extent of a low frequency source needs to be determined, classical TR cannot give access to this

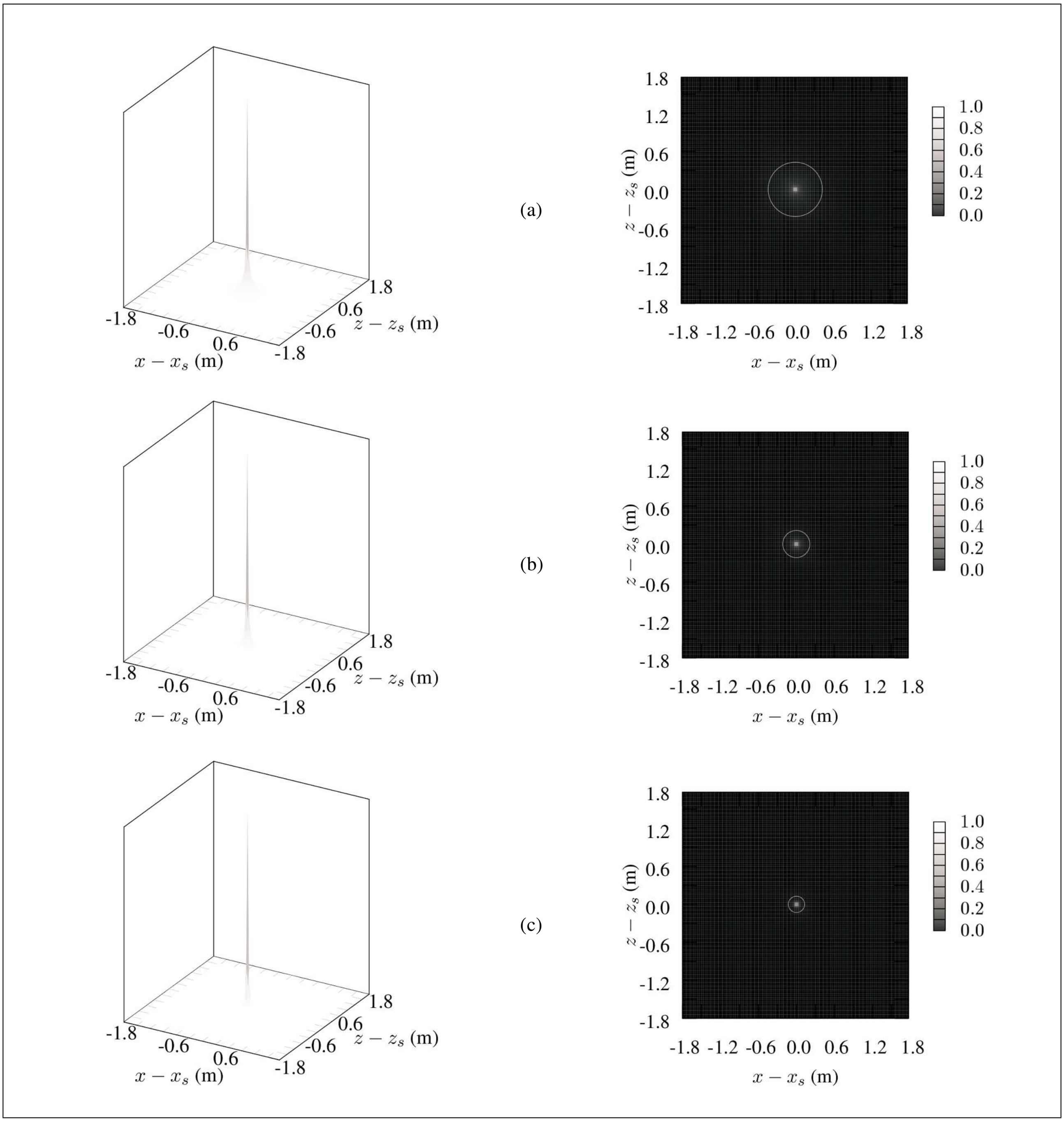

Figure 5. Imaging of a underwater pointlike sound source in the SOFAR channel using the numerical time reversal sink method at central frequencies of (a) 1500 Hz, (b) 3000 Hz, and (c) 5000 Hz. Left: squared acoustic pressure. Right: Source imaging (grayscale) compared to the theoretical limit of resolution (circles).

information because the classical TR process does not recreate the exact time-reversed field since the source singularity is not time-reversed, and the diffraction effects lead to limited resolution localization.

It is important to note that the propagation properties of the medium (in terms of sound velocity) must be known. But, in most underwater applications, this profile can be accessed with conductivity-temperature-depth probes. This numerical experiment shows that the numerical TRS imaging method is very accurate and can be used in high definition acoustic source detection and characterization in underwater applications. The limits of this method are that the sound velocity profile and the measurement array position must be known accurately [31], even though Kuperman *et al.* [27] already showed that the time reversal techniques are relatively robust to temperature change and array position for classical TR underwater communications. The technique used in TR communications is exactly the same as in numerical TR localization, instead that the backpropagation is done in the real channel. The numerical TRS imaging method being a refinement of TR localization, the limits in terms of stability

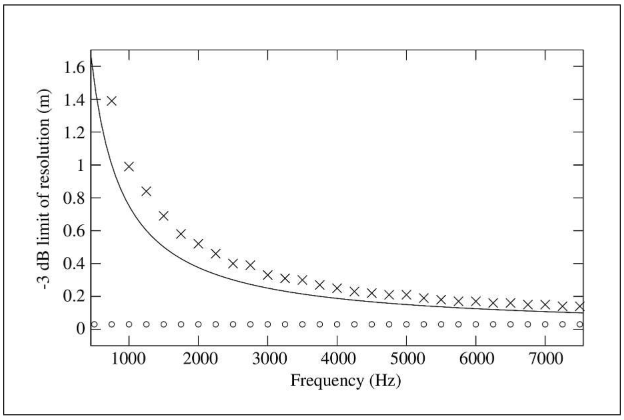

Figure 6. Space resolution of the TR process (cross) and the numerical TRS imaging (circles) in the SOFAR channel compared to the classical half-wavelength diffraction limit of resolution (solid line) for the frequencies computed in the numerical experiment.

when the propagation channel properties and array position change are basically the same.

4. Experimental results and discussion

4.1. Imaging of a single sound source in an anechoic room using a numerical TRS

In this Section, we present experimental results of acoustic imaging of real active sources in an anechoïc room, as described in Section 2.1. These sources are 5.08 cm diameter / 15-Watt electrodynamic transducers, that emit an impulsive signal (2.5-cycles Blackman windowed sinusoid at several central frequencies, from 300 Hz to 8000 Hz) in the room at several arbitrary positions. The localization obtained using numerical TR backpropagation and TRS imaging are then computed using sound pressure measurements at 36 control points distributed on a 2-D microphone array with equal inter-microphone spacing of 75 mm. For each experiment, the exact sound velocity has been measured with a time of flight experiment, in order to calibrate the numerical simulation of the sound propagation involved in the classical TR and the numerical TRS imaging process and to avoid any errors in the propagation simulation due to temperature variations.

Figure 7 shows the source localization achieved with the numerical TR backpropagation, for two different source positions, at a central frequency of 750 Hz. Each subfigure shows a gray scale image and a 3-dimensional mesh showing the normalized quadratic acoustic pressure in a vertical plane including the source, using numerical TR backpropagation. The first source is located on a line passing through the array center and perpendiculat to the array, 35 cm from the array center "on-axis source"), and the second source is located in the same plane parallel to the array as the first source, at 29 cm from the line passing through the array center and perpendicular to the array ("off-axis source").

The two sources are well localized by numerical TR backpropagation, despite the fact that the number of monitoring microphones is low: the focal point corresponds exactly to the position of the source in the experiment, determined by distance measurement between the source and 3 points on the microphone array during the experiment and calculated by triangulation using these distance measurements. Nevertheless, it is important to note that TR reconstruction for the source located away from the array aperture is very asymmetric: the sound field is not as well reconstructed outside the microphone array aperture, although the maximum corresponds exactly to the real position of the acoustic source. This shows that this method based on numerical TR backpropagation is applicable (though less accurate) when the source position is not in the array aperture. The acoustic maps obtained via numerical TR backpropagation give information on the position of the sound sources in the anechoic room, but the size of the focal spot is not related to the actual size of these sources, and the resolution is limited by diffraction effects. As predicted by theory, classical TR only allows to localize the sources. All the information about the sources is included in the acoustic field measured by the TRM, but the TR process does not re-create the exact time-reversed field because the source singularity is not time-reversed.

Figure 8 shows that the time signal obtained by numerical TR at the source position is equally well reconstructed at the source position even if the source is away from the array aperture. This means that the numerical TRS imaging is likely to be effective in both cases even if the TR reconstruction is not adequate around the source because this high resolution imaging process requires the acoustic pressure to be well reconstructed at the source position [11, 13].

The data obtained from TR numerical reconstruction are then linearly combined to the soundfield of a numerical time-reversal sink that emits the "antinoise" signal at the position of the source localized by TR reconstruction. The results obtained after this computation are presented on Figure 9. This Figure shows a grayscale image of the reconstructed sound sources in the anechoic room (in the $x = 35$ cm vertical plane) and a 3-dimensional mesh showing the normalized squared acoustic pressure using the numerical time-reversal sink. The circles superposed on the images indicate the actual size of the loud speaker membrane. This experiment shows that the sound sources are well localized thanks to TR, and that the physical size of the transducers is very well reconstructed by the numerical TRS technique.

Even with a small number of measurement microphones and for a source outside the measurement array aperture, the imaging achieved has subwavelength resolution. This allows satisfactory source imaging without the need of scanning the entire medium. This new imaging technique appears to be a very efficient alternative to other acoustic imaging processes (beamforming and nearfield acoustic holography) in open space, with a few transducers, when the propagation medium is well known. Finally, it is im-

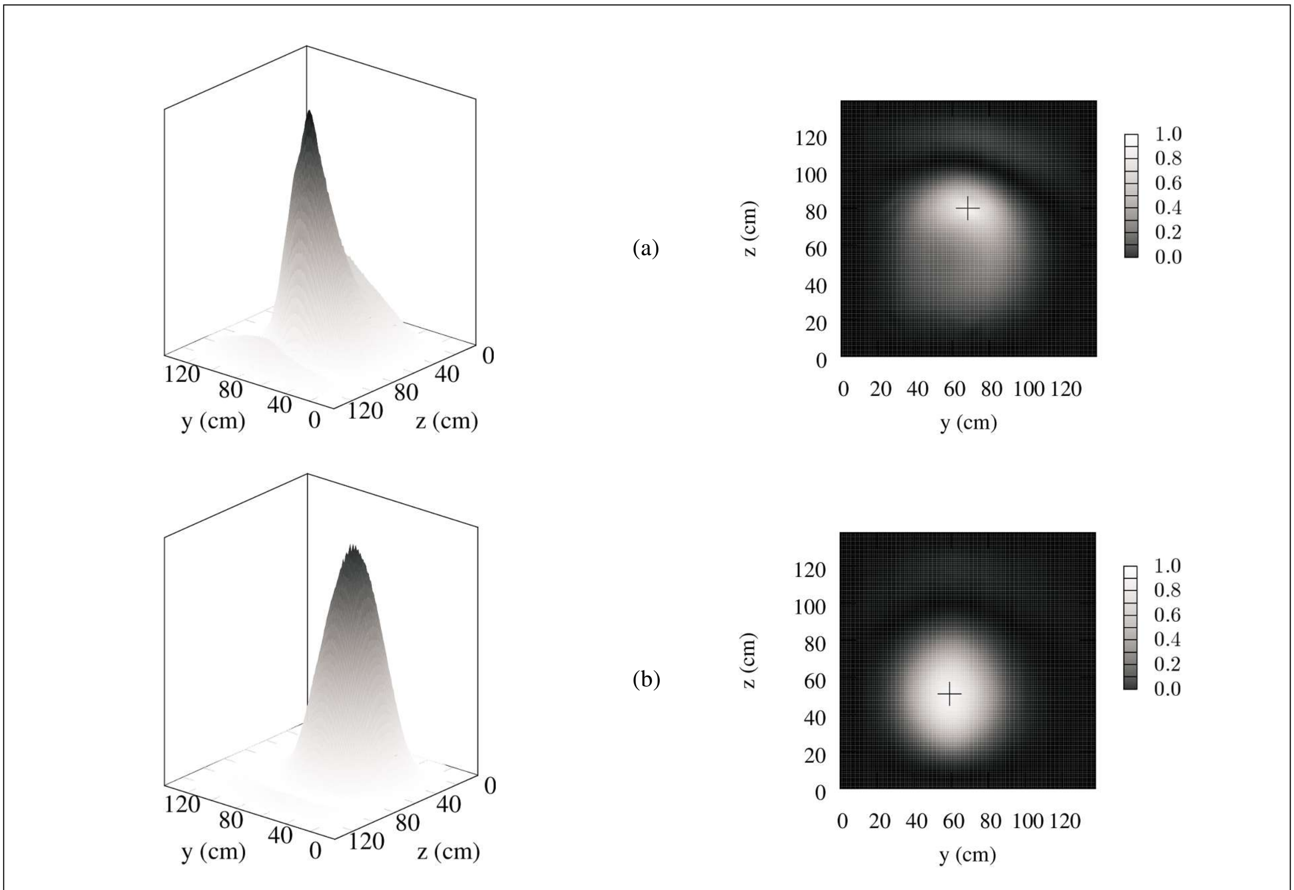

Figure 7. Localization of a 5.08 cm diameter acoustic source using numerical TR backpropagation, at central frequency of 750 Hz (a) off-axis source and (b) on-axis source. The two sources are in a plane (z, y), parallel to the microphone array, located at 35 cm from the array. Left: normalized squared acoustic pressure. Right: Source localization (grayscale). The real position of the source is shown (cross).

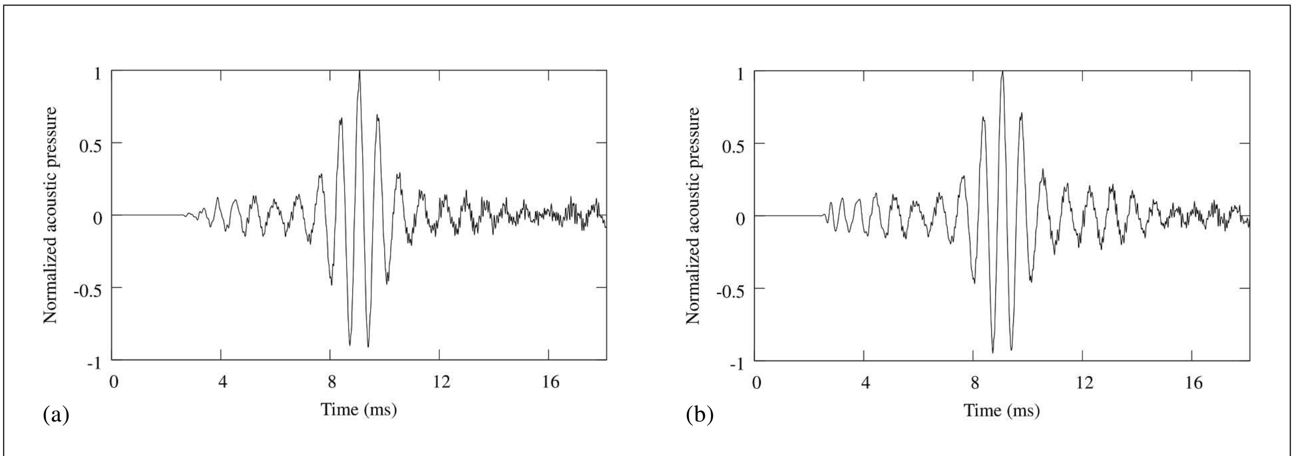

Figure 8. Normalized acoustic pressure at the source position extracted from TR computation, for the 5.08 cm diameter source at central frequency of 750 Hz, (a) off-axis source and (b) on-axis source. These signals correspond to the “antinoise” signals used in the TRS process.

portant to note that in these experiments, the TRS imaging shows slightly smaller size than the actual size of loudspeaker membrane (see Figure 10). This can be explained by the source reconstruction involved: the TRS process reconstructs the actual pressure distribution of the transducers in the anechoic room, which is not uniform on the membrane surface. Thus, the TRS imaging reconstructs this actual source distribution and the size of the transducer is slightly underestimated. Nevertheless, the results obtained with the numerical TRS method provides high-

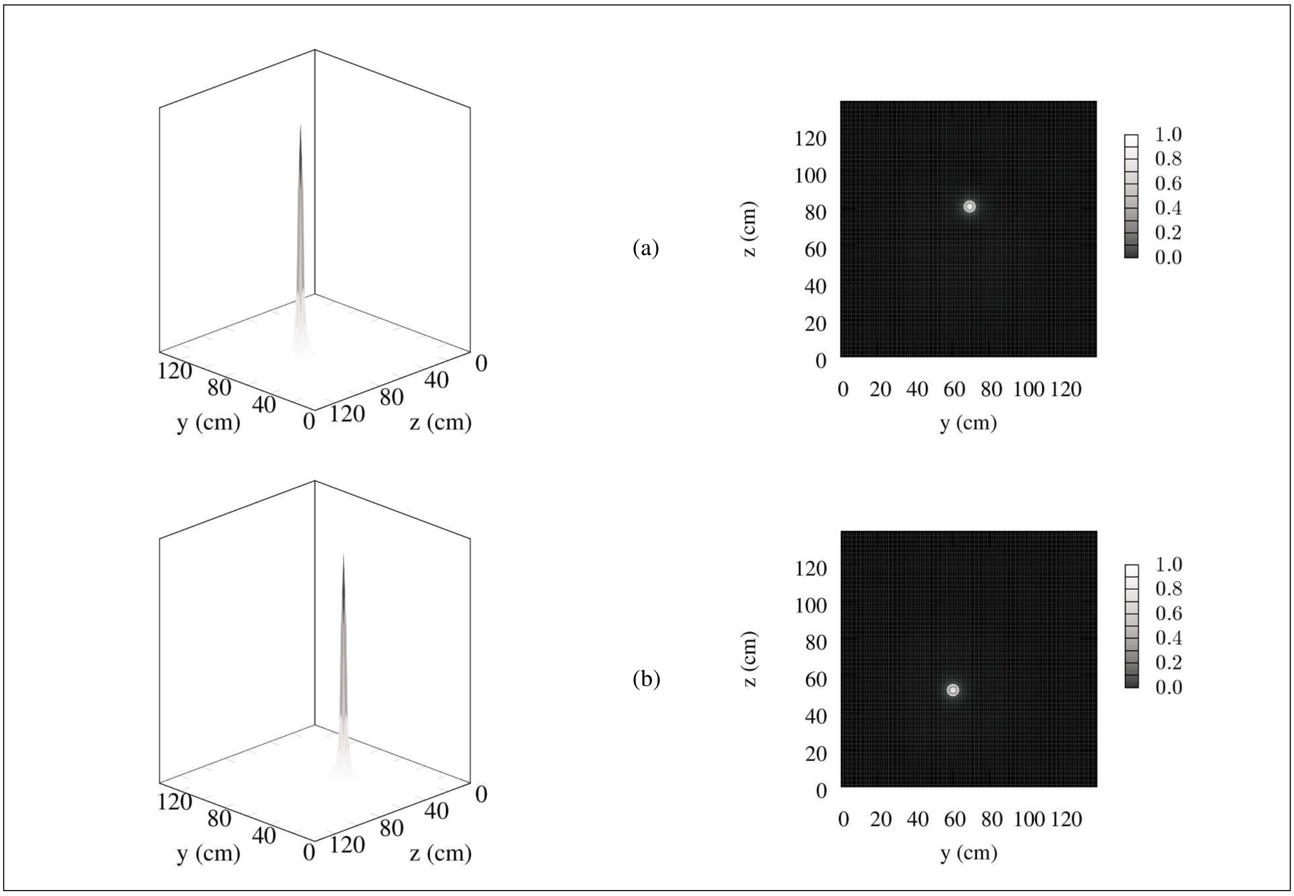

Figure 9. Numerical TRS imaging of a 5.08 cm diameter acoustic source at central frequency of 750 Hz (a) off-axis source and (b) on-axis source. The two sources are in a plane (z, y), parallel to the microphone array, located at 35 cm from the array. Left: normalized squared acoustic pressure. Right: Source localization (grayscale). The real size of the source is plotted at the source position (circle).

resolution imaging of active sound sources in free field with only a few transducers, provided that the wave propagation in the medium is accurately modeled.

4.2. Simultaneous imaging of several sound sources in an anechoïc room using a numerical TRS

4.2.1. Simultaneous imaging of two incoherent sound sources

Figure 11 shows the ability of the numerical TRS method to simultaneously image two acoustic sources that emit different signals with different frequency contents. In this experiment conducted in the anechoic room, two 5.08 cm diameter transducers emit a 1.5-cycles blackman windowed sinusoid respectively at 950 Hz and 1450 Hz. These two sources are separated by 41 cm. The two sources emit their signal simultaneously, and the resulting acoustic field is measured by the 36 control microphones of the measurement array. The numerical TR backpropagation and numerical TRS imaging are then computed using the same simulation grid than the one presented previously. Figure 11 shows the localization achieved by numerical TR backpropagation and the imaging achieved using the numerical TRS method, at collapse time.

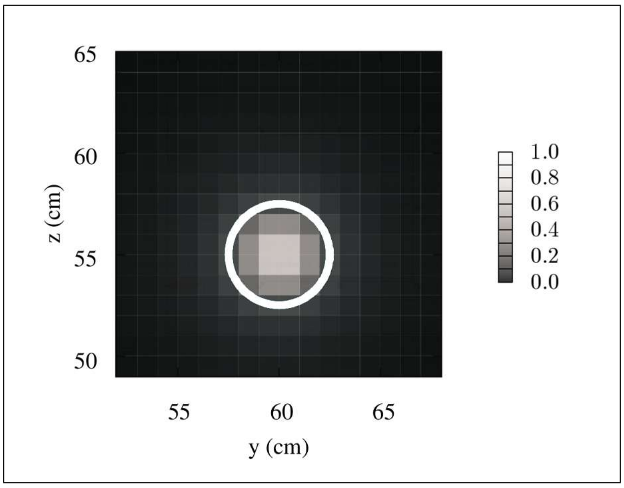

Figure 10. Zoom on the numerical TRS imaging of the 5.08 cm diameter acoustic source at central frequency of 750 Hz. This zoom shows the real size of the transducer (circle), and the discretization cell.

These data show that the numerical TRS imaging is very efficient even with several sources emitting different signals. In this figure, the two sources are well imaged and their size is well determined by the method, even if the fre-

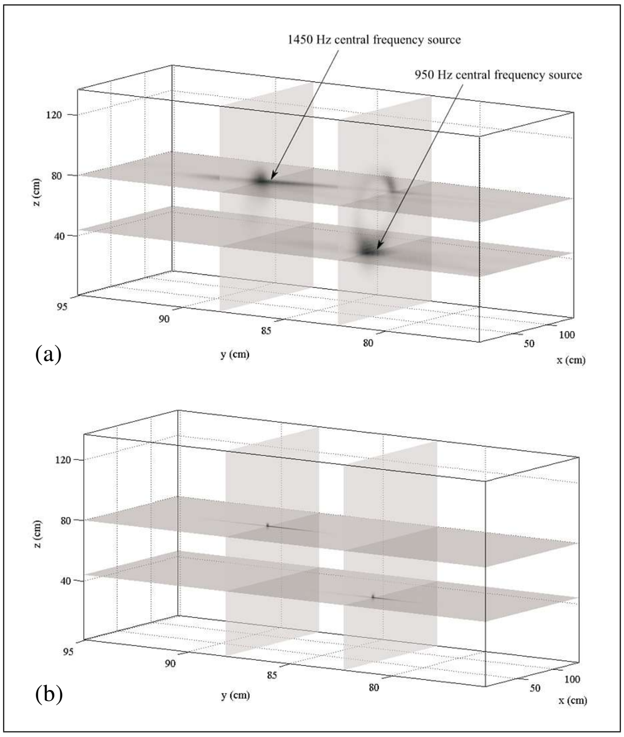

Figure 11. (a) Numerical TR backpropagation at collapse time; (b) Numerical TRS imaging at collapse time for two loudspeakers emitting simultaneously a 1.5-cycles blackman windowed sinusoid, respectively at central frequency of 950 Hz and 1450 Hz.

quency content of the two emitted signals is different. This result confirms that the numerical TRS is a very accurate imaging method and provides an efficient refinement to classical TR for acoustic sources detection and imaging. It is important to note that the TR localization is perturbated by the presence of another source, because the spatial extent of the TR focusing depends on the signal wavelength. The TRS method achieves high resolution imaging without any perturbation from other sources, because the TRS method recreates the exact time-reversed situation of the initial sound emission, whereas TR method does not.

4.2.2. Super-resolution imaging of three sources localised within the diffraction limit using TRS and MUSIC

In this experiment, the numerical TRS method is used to image simultaneously three loudspeakers emitting a 1.5-cycles blackman windowed sinusoid. Two of them emit a signal at the same frequency (500 Hz) and the third one emits a signal at 650 Hz. The three loudpseakers are located on the vertices of an equilateral triangle whose sides are 10 cm. The resulting acoustic field is measured by the 36 control microphones of the measurement array. The numerical TR backpropagation of these measurements is shown on Figure 12. In this particular configuration, it is impossible to separate the three sources with a spatio-temporal maximum detection.

However, it is possible to determine the position of the three sources using the a high-resolution algorithm, such as MUSIC [32], or ESPRIT [33]. These methods allow to determine the center of the three loudspeakers, using a decomposition of the signal representation in two orthogonal spaces: the noise subspace and the signal subspace. Nevertheless, the spatial pseudospectrums obtained using these methods only allow to localize the sources, without any information on their boudaries nor on their spatial extent.

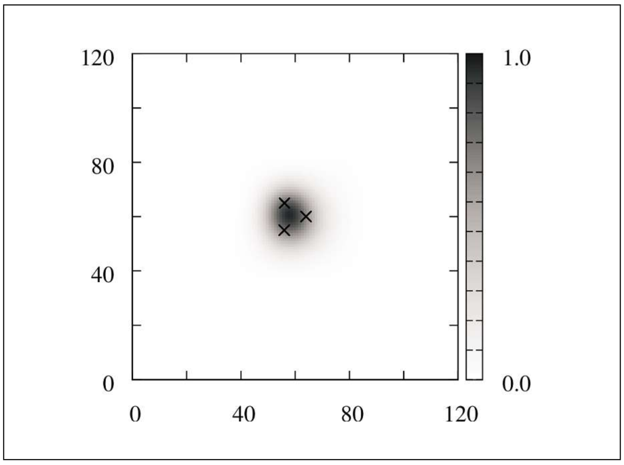

Figure 12. Numerical TR backpropagation of three loudspeakers within the diffraction limit. The position of the three sources is plotted for reference (cross).

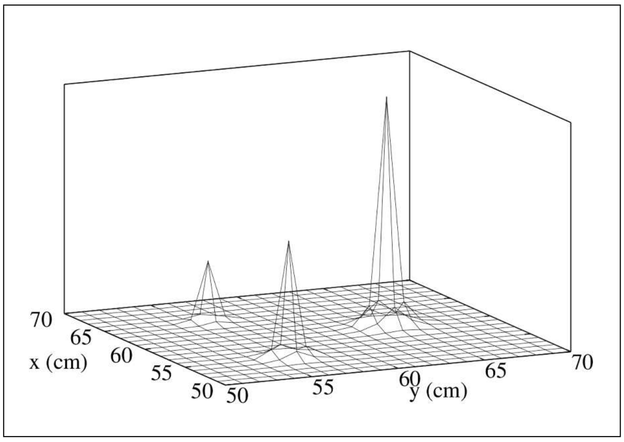

Figure 13. MUSIC Spatial pseudospectrum of the data measured by the 36 control microphones: the centers of the three loudspeakers are well resolved within the diffraction limit.

Figure 13 shows the spatial MUSIC pseudospectrum obtained with the data measured by the 36 control microphones. Thus, the MUSIC method allows to determine the position of the three sources.

The TRS signal is then extracted at these positions from the computed TR backpropagation. Figure 14 shows the numerical TRS super-resolution imaging computed using three sources, located at the positions extracted from the MUSIC algorithm and the temporal signals extracted from the TR backpropagation. This figure shows that MUSIC and TRS allow super-resolution imaging of the three loudspeakers obtained with the TRS technique, and give high-resolution information on both the position and the size of the loudspeakers, whereas classical TR backpropagation fails.

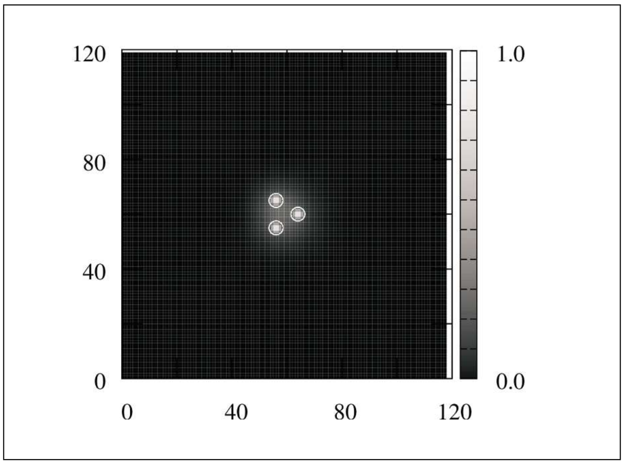

Figure 14. Super-resolution imaging of three sources localised within the diffraction limit with the combination of the MUSIC localization method and the numerical TRS method. The real size of the source is plotted at the source position (circles).

In this particular case, the spatio-temporal maximum detection has been replaced by a spatial MUSIC localization, and the numerical TRS imaging process has been used to determine the spatial boundaries of the three sources. It is important to note that the method does not depend on the frequency content of the sources, and that the numerical TRS method allows to achieve super-resolution imaging where other techniques such as classical TR backpropagation and beamforming fail.

5. Conclusions

In this paper, we have shown that a numerical time-reversal sink (TRS) can be used to achieve high resolution imaging of active sound sources in open space. These results extend to three dimensional acoustics the work previously published by the authors in [10] for flexural waves in a dispersive clamped plate. In the present case, the numerical TRS imaging method has been applied to audible sound sources in a three-dimensional open space. As the numerical TRS method relies on a model of the sound propagation in the medium, a finite difference model has been derived in order to simulate the propagation of acoustic waves in a three dimensional layered medium. An application to underwater acoustic sources imaging has been presented as a proof of concept and the experimental imaging of real acoustic transducers in audible range in an anechoic room has been demonstrated. The numerical TRS imaging proves to be an efficient imaging technique, giving access to high resolution imaging of the the actual source distribution in audible range and giving information on the position and size of the active sound sources, even if these sources are located away from the measurement array aperture. It has been shown that the numerical TRS techniques allows to achieve high resolution imaging instead of limited resolution localization of acoustic sources, even when several sources are emitting different signals simultaneously. The numerical TRS may be a good alternative to other acoustic imaging process, giving rise to interesting potential applications that need to be studied, in underwater acoustics, musical acoustics, and source identification of industrial structures.

Acknowledgments

The authors would like to thank Jean-Dominique Polack (IJLRA/LAM, Paris, France), Vincent Gibiat (PHASE, Toulouse, France), Yann Pasco (GAUS, Sherbrooke, Canada), Steve Allen (CCS, Sherbrooke, Canada) and Charles Besnainou (IJLRA/LAM, Paris, France) for useful discussions and friendly comments on experimental work and numerical simulations.

References

[1] J. D. Maynard, E. G. Williams, Y. Lee: Nearfield acoustic holography: I. Theory of generalized holography and the development of NAH. J. Acoust. Soc. Am. **78** (1985) 1395–1413.

[2] N. O. Booth, P. Baxley, J. A. Rice, P. W. Schey, W. S. Hodgkiss, G. L. D'Spain: Source localization with broadband matched-field processing in shallow water. IEEE J. Ocean Eng. **21** (1996) 402–12.

[3] C. Prada, J. L. Thomas, M. Fink: The iterative time reversal process: Analysis of convergence. J. Acoust. Soc. Am. **97** (1995) 62–71.

[4] C. Prada, S. Manneville, D. Spoliansky, M. Fink: Decomposition of the time reversal operator: Detection and selective focusing on two scatterers. J. Acoust. Soc. Am. **99** (1996) 2067–2076.

[5] S. K. Lehman, A. J. Devaney: Transmission mode time-reversal super-resolution imaging. J. Acoust. Soc. Am. **113** (2003) 2742–2753.

[6] A. Sutin, P. Johnson, J. Tencate, A. Sarvazyan: Time reversal acousto-seismic method for land mine detection. Conference on Detection and Remediation Technologies for Mines and Minelike Targets 5794, 2005, 706–716.

[7] M. D. Collins, W. A. Kuperman: Focalization: Environmental focusing and source localization. J. Acoust. Soc. Am. **90** (1991) 1410–1422.

[8] J. M. Parot: Localizing impulse sources in an open space by time reversal with very few transducers. Appl. Acoust. **69** (2008) 311–324.

[9] M. Fink, D. Cassereau, A. Derode, C. Prada, P. Roux, M. Tanter, J. L. Thomas, F. Wu: Timereversed acoustics. Rep. Prog. Phys. **63** (2000) 1933–1995.

[10] E. Bavu, A. Berry, J. D. Polack: Super-resolution imaging of active vibrational sources using a time-reversal sink. J. Sound Vib. (2009) submitted.

[11] J. de Rosny, M. Fink: Overcoming the diffraction limit in wave physics using a time-reversal mirror and a novel acoustic sink. Phys. Rev. Lett. **89** (2002) 24301–1–124301–4.

[12] J. de Rosny: Milieux réverbérants et réversibilité. PhD Thesis, Laboratoire Ondes et Acoustique, ESPCI, Université Paris VII, 2000.

[13] E. Bavu, C. Besnainou, V. Gibiat, J. de Rosny, M. Fink: Subwavelength sound focusing using a time-reversal acoustic sink. Acta Acustica united with Acustica **93** (2007) 706–715.

[14] C. Draeger, M. Fink: One channel time-reversal of elastic waves in a chaotic 2D-silicon cavity. Phys. Rev. Lett. **79** (1997) 407–410.

[15] C. Draeger, J.-C. Aime, M. Fink: One-channel time-reversal in chaotic cavities: Experimental results. J. Acoust. Soc. Am. **105** (1999) 618–625.

[16] E. Habets: Single and multi microphone speech dereverberation using spectral enhancement. PhD Thesis, Technische Universiteit Eindhoven, 2007.

[17] N. S. Krylov: Works on the foundations of statistical physics. Princeton University Press, 1979.

[18] F. H. Van den Dungen: Acoustique des salles. Gauthier-Villars, 1934.

[19] D. Cassereau, M. Fink: Time-reversal of ultrasonic fields. Part III: Theory of the closed time-reversal cavity. IEEE Trans. Ultrason. Ferroelec. Freq. Contr. **39** (1992) 579–592.

[20] A. Sei: Étude de schémas numériques pour les modèles de propagation d'ondes en milieu hétérogène. PhD Thesis, Université Paris IX-Dauphine, 1991.

[21] G. C. Cohen: Higher-order numerical methods for transient wave equations. Springer Verlag, 2002.

[22] S. Hairer, P. Norsett, G. Vanner: Solving ordinary differential equations. Springer Series in Computationnal Mathematics, 1991.

[23] M. A. Dablain: The application of high-order differencing for the scalar wave equation. Geophysics **51** (1986) 54–66.

[24] F. Collino: High order absorbing boundary conditions for the 3D wave equation. Inria research report No. 2932, ISSN 0249-6399, 1996.

[25] F. Collino: High order absorbing boundary conditions for wave equation models in rectangular domains. Inria research report No. 1790, Inria-00077030, 1992.

[26] Higher order paraxial wave equation approximations in heterogeneous media. Part II. Inria research report No. 558, 1986.

[27] H. C. Song, P. Roux, W. S. Hodgkiss, W. A. Kuperman, T. Akal, M. Stevenson: Multiple-input/ multiple-output coherent time reversal communications in a shallow water acoustic channel. IEEE J. Oceanic Eng. **31** (2006) 170–178.

[28] G. F. Edelmann, T. Akal, W. S. Hodgkiss, S. Kim, W. A. Kuperman, H. C. Song: An initial demonstration of underwater acoustic communication using time reversal. IEEE J. Ocean. Eng. **27** (2002) 602–609.

[29] P. Roux, M. Fink: Time reversal in a waveguide: Study of the temporal and spatial focusing. J. Acoust. Soc. Am. **107** (2000) 2418–2429.

[30] R. C. Spindel: Sound transmission in the ocean. Annual Review of Fluid Mechanics **17** (1985) 217–237.

[31] M. E. Anderson, M. S. McKeag, G. E. Trahey: The impact of sound speed errors on medical ultrasound imaging. J. Acoust. Soc. Am. **107** (2000) 3540–3548.

[32] Y. D. Huang, M. Barkat: Near-field multiple source localization by passive sensor array. IEEE Trans. Antennas Propag. **39** (1991) 968–975.

[33] R. Roy, T. Kailath: ESPRIT – Estimation of signal parameters via rotational invariance techniques. IEEE Trans. Acoust. Speech Signal Processing **37** (1989) 984–995.